Multifunctional characteristics of $BaNb_{0.3}Ti_{0.7}O_3$/Si *p-n* junctions

Yanhong Huang, Kun Zhao, Huibin Lu,[a] Kui-juan Jin, Meng He, Zhenghao Chen, Yueliang Zhou, and Guozhen Yang
Beijing National Laboratory for Condensed Matter Physics, Institute of Physics, Chinese Academy of Sciences, Beijing 100080, People's Republic of China

(Received 17 October 2005; accepted 28 December 2005; published online 10 February 2006)

$BaNb_{0.3}Ti_{0.7}O_3$/Si *p-n* junction combining the functional properties of oxide and Si electronics was fabricated by laser molecular-beam epitaxy, and the multifunctional properties of rectification, ferroelectricity and photoelectricity were experimentally studied. The good rectifying *I-V* characteristics, nanosecond ultrafast photoelectric effect, and ferroelectric property due to the interface enhancement were observed experimentally. The mechanisms of ferroelectric behavior and photoelectric process are discussed briefly. © *2006 American Institute of Physics*.
[DOI: 10.1063/1.2172290]

Barium titanate ($BaTiO_3$) is one of the most extensively investigated perovskite oxide materials because of its remarkable ferroelectric, dielectric, pyroelectric, electro-optical, and nonlinear optical properties.[1–5] $BaTiO_3$ thin films have attracted much attention for their potential applications. A large number of papers have been focused on the fabrication and properties of $BaTiO_3$ thin films as well as the structural, electrical, and optical properties of Nb-doped $BaTiO_3$ thin films.[6–12] Mckee *et al.* have epitaxially grown $BaTiO_3$ thin film on Si substrate.[13] However, to our knowledge, as a basic element for application, $BaTiO_3$ *p-n* junction has not been reported anywhere other than in our previous paper on the rectifying current-voltage (*I-V*) characteristics of $BaTiO_3$ *p-n* junctions.[14] In this letter, we will report the results of research on the multifunctional properties of rectification, ferroelectricity and photoelectricity of $BaNb_{0.3}Ti_{0.7}O_3$ (BNTO) and Si *p-n* junctions.

The BNTO/Si *p-n* junctions were fabricated by a computer-controlled laser molecular-beam epitaxy (laser MBE) system equipped with *in situ* reflection high-energy electron diffraction (RHEED).[15] In order to fabricate high-quality BNTO thin films on Si substrates and form better *p-n* interface, we used the two-step method to epitaxially grow the BNTO thin film on Si substrate as described in our previous work.[16] Firstly, about two-unit-cell thick BNTO film was deposited on the substrate surface at room temperature with a base pressure of 3×10^{-6} Pa in epitaxial chamber. Then, the Si substrate was heated to 620 °C and annealed. After the RHEED streak pattern of the initial two-unit-cell thick BNTO film appeared, the BNTO was continuously deposited under the O_2 pressure of 6×10^{-4} Pa with the substrate temperature kept at 600 °C during the deposition. The BNTO film with thickness of about 300 nm was deposited with a growth rate of about one unit-cell layer per 35 pulses.

Figure 1 shows a typical x-ray diffraction (XRD) θ-2θ scan pattern of 300 nm BNTO film on Si substrate. BNTO (001), (002), and Si (200), (400), and there was no diffraction peaks from impurity phases or randomly oriented grains. The RHEED pattern of 300 nm BNTO on Si substrate is shown in the inset of Fig. 1. The results of *in situ* RHEED and *ex situ* XRD in Fig. 1 indicate that the BNTO film is single phased and epitaxially grown on the Si substrate.

The *I-V* characteristics of the BNTO/Si *p-n* junction were measured by a pulse-modulated current source at room temperature. The schematic circuit is shown in the left inset of Fig. 2. Our measurement shows that the leakage current in the reverse bias region is about 0.06 mA at −2 V and the ratio of forward and reverse currents reaches 110 in the applied voltage region from −2 to 2 V. In order to investigate the transport phenomenon, the resistance as a function of temperature for the BNTO film was measured by four-probe technique. The R-T curve of BNTO thin film is shown in the right inset of Fig. 2. The BNTO thin film exhibits a metal-like behavior from 5 to 300 K. The carrier concentrations of BNTO film and Si substrate are 1.55×10^{17} cm^{-3} and 1.45×10^{15} cm^{-3} by Hall measurement, respectively. Based on the above results, the *I-V* characteristics shown in Fig. 2 are dominated by the *p-n* junction.

The most interesting property of the *p-n* junction is the ferroelectricity. The polarization versus electric field (*P-E*) hysteresis loops were measured with RT6000S ferroelectric test system in virtual ground model at ambient temperature. Figure 3 shows the *P-E* hysteresis of BNTO/Si *p-n* junction, in which an increased reverse field was applied at the beginning of the measurement. The remnant polarization (P_r) and coercive field (E_c) for the junction are 1.78 $\mu C/cm^2$ and 278 kV/cm, respectively. The hysteresis loop is not closed as a function of electric field. The possible reason is the asymmetrical space charge near the interface of the *p-n*

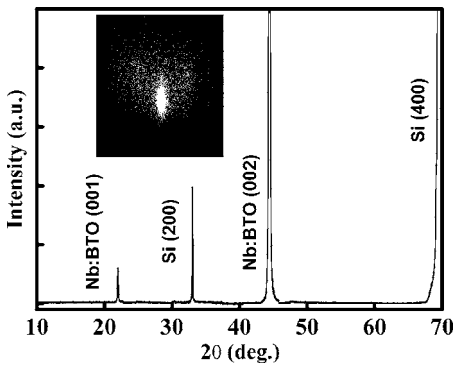

FIG. 1. XRD θ-2θ scan curve of 300 nm thick BNTO film on Si substrate. The inset shows RHEED pattern of BNTO film.

[a]Author to whom correspondence should be addressed; electronic mail: hblu@aphy.iphy.ac.cn

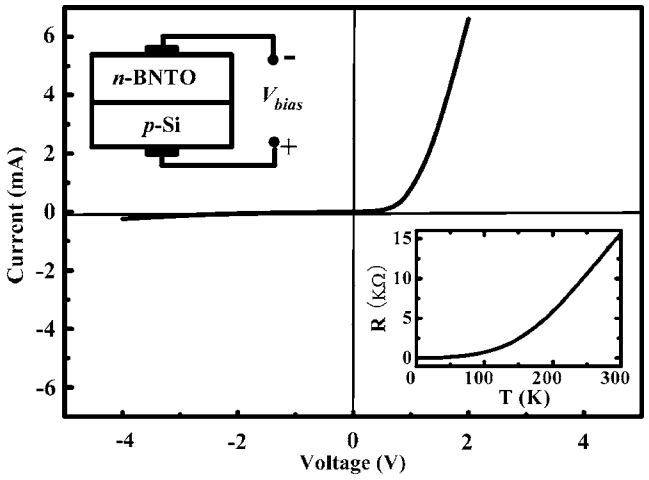

FIG. 2. *I-V* curve of the BNTO/Si *p-n* junction at the room temperature. The top inset shows the schematic circuit of the sample measurement and the bottom one is the resistance vs temperature curve of BNTO thin film.

junction.[17,18] In the heterostructure of *n* doped BNTO and *p* doped Si, a polarization of space charges is formed perpendicular to the interface due to the electrons in Si diffused from BNTO and the holes left in BNTO near the interface of the *p-n* junction. If we starte our measurement with an increased reverse field, the built-in field of the system will be enhanced, as well as the polarization. Thus, with *E* perpendicular to the interface, the hysteresis loop mainly results from the space charges in the depletion layer of the *p-n* junction. It is worthy to note that we have not observed the *P-E* loop in the BNTO thin film due to the higher Nb-doping (30%) and very large leakage current. This fact gives a support for the enhanced ferroelectricity originating from the junction interface. The detailed mechanism needs further investigation.

The photoelectric behavior of BNTO/Si *p-n* junction (2 mm×4 mm) was further investigated using a 1064 nm Nd: YAG laser (pulse width 25 ps) with the energy density of 1 mJ/cm^2 and measured by a 500 MHz digital oscilloscope (Tektronix TDS3052B). Similar to $La_{0.7}Sr_{0.3}MnO_3$/Si and $SrTiO_{3-\delta}$/Si *p-n* junctions,[16,19] as shown in Fig. 4, a photovoltaic pulse has been observed with a rise time of ~380 ps (10%–90%) and a full width at half maximum (FWHM) of 2 ns when a 5 Ω resistance was connected in parallel with the *p-n* junction and the BNTO film surface was irradiated by a laser pulse. The FWHM of the photovoltaic pulse should actually be narrower because the oscilloscope has limited bandwidth of 500 MHz in our experiment.

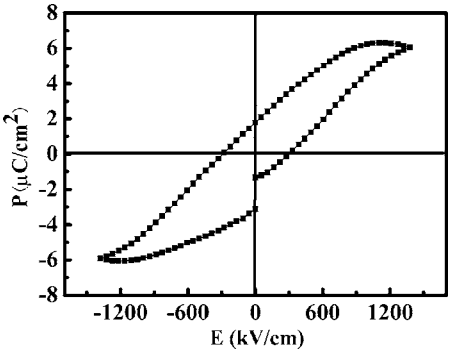

FIG. 3. Ferroelectric hysteresis loop of the BNTO/Si *p-n* junction.

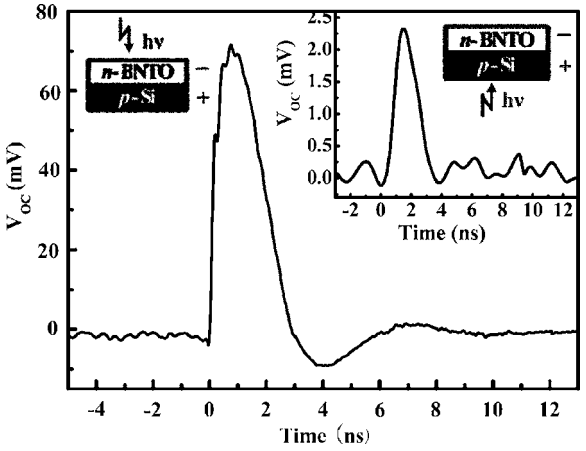

FIG. 4. Variation of the transient photovoltage in the*p-n* junction with time when irradiated from the BNTO side and the Si side (the inset) by 1064 nm laser pulses, respectively.

For better understanding of the photovoltaic effects of the BNTO/Si *p-n* junction, we have also measured the photovoltaic pulse when the Si substrate was irradiated by a laser pulse under the same condition as Fig. 4. As shown in the inset of Fig. 4, the magnitude of the photovoltaic pulse was decreased 30 times when the laser was irradiated through the Si substrate rather than through the BNTO film.

Figure 5 shows the absorption spectra of the BNTO/Si and the clean Si substrate used for the BNTO film growth. The measurements were taken at the wavelength range of 650–2600 nm using a FTS 6000 spectrophotometer. It can be seen that a striking absorption occurs near the 1024 nm wavelength (1.2 eV), maybe resulting from the intermediate levels in the forbidden gap induced by Nb doping or oxygen deficiency which play the role of trapping centers.[20] The laser of wavelength 1064 nm (1.16 eV) is absorbed in the BNTO film with an absorption length of α^{-1}, which is larger than BNTO film thickness in our sample, allowing some 1064 nm laser to pass through the BNTO film to the Si substrate. The inset in Fig. 5 shows the schematic band structure of the BNTO/Si *p-n* junction under the 1064 nm laser irradiation. The photovoltaic process can be understood as follows. When BNTO film is connected with Si, electrons from BNTO and holes from Si will diffuse into the opposite sides,such that a diffusion barrier is built up around the in-

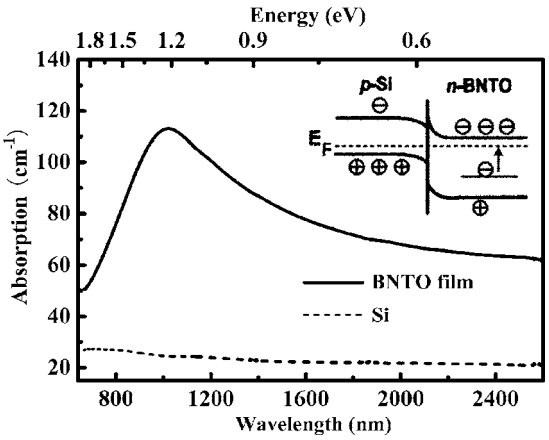

FIG. 5. Absorption spectra of the Si substrate (broken lines) and the BNTO film on the Si substrate (solid lines). The inset shows the band structure of the BNTO/Si *p-n* junction under the 1064 nm laser irradiation.

terface, making the carriers in equilibrium on the two sides. Under the 1064 nm laser irradiation, the photons are absorbed to create the photoinduced carriers in both BNTO film and Si (band gap is ~1.1 eV) substrate. In the case of BNTO films, the band-to-interband excitation takes place first, generating nonequilibrium carriers which will be captured by the trapping centers in the gap. Then these trapped carriers will be excited once more by the incident laser and will be transferred into the conduction band. Therefore, near the interface of the *p-n* junction, photoinduced electrons in conduction band of Si will drift into the conduction band of BNTO film under the built-in field, meanwhile, photoinduced holes in valence band of BNTO will drift into the valence band of Si, eventually leading to the occurrence of a transient photovoltage. Furthermore, when the Si substrate of the junction is irradiated by the same laser pulse, the photoinduced carriers which can diffuse into the interface region are very few in comparison with that incident from BNTO films since the thickness of Si (~0.4 mm) is much larger than the drift length of nanometer order,[21] so it is reasonable that only the 2.3 mV photovoltaic signal was observed in the inset of Fig. 4.

In summary, we have fabricated high-quality BNTO/Si *p-n* junctions and observed the good rectifying *I-V* characteristics, ultrafast photoelectric effects, and ferroelectric property. It is noteworthy that the interface of the *p-n* junction can enhance the ferroelectric property even if the ferroelectric property is not good enough because the ferroelectric property is not present in the higher Nb-doped BNTO film. Further research on improving the ferroelectricity by changing Nb-doping concentration and growth conditions, and investigation on the mechanism behind the interesting phenomena are under way.

This work is supported by the National Natural Science Foundation of China (Grant Nos. 10334070 and 60576015) and the National Key Basic Research and Development Program of China (Grant No. 2004CB619004).

[1] N. K. Kim, S. G. Yoon, W. J. Lee, and H. G. Kim, J. Mater. Res. **12**, 1160 (1997).
[2] D. Geschke, N. Leister, M. Steffen, H. J. Glasel, and E. Hartmann, J. Mater. Sci. Lett. **16**, 1943 (1997).
[3] K. Nashimoto, D. K. Fork, F. A. Ponce, and J. C. Tramontana, Jpn. J. Appl. Phys., Part 1 **32**, 4099 (1993).
[4] M. Sayer and K. Sreeniras, Science **247**, 1056 (1990).
[5] R. E. Chen, Nature (London) **358**, 136 (1992).
[6] H. Shigetani, K. Kobayashi, M. Fujimoto, W. Sugimura, Y. Matsui, and J. Tanaka, J. Appl. Phys. **81**, 693 (1997).
[7] D. F. Cui, H. S. Wang, Z. H. Chen, Y. L. Zhou, H. B. Lu, G. Z. Yang, K. Ma, H. Chen, L. Li, W. Liu, and Y. Zhang, J. Vac. Sci. Technol. A **15**, 275 (1997).
[8] S. R. Gilbert, L. A. Wills, B. W. Wessels, J. L. Schindler, J. A. Thomas, and C. R. Kannewurf, J. Appl. Phys. **80**, 969 (1996).
[9] L. Yan, H. B. Lu, Z. H. Chen, S. Y. Dai, Y. L. Zhou, and G. Z. Yang, J. Cryst. Growth **244**, 255 (2002).
[10] K. Kowalski, M. Ijjaali, T. Bak, B. Dupre, J. Nowotny, M. Rekas, and C. C. Sorrell, J. Phys. Chem. Solids **62**, 543 (2001).
[11] L. F. Liu, H. Z. Guo, H. B. Lu, S Y Dai, B. L. Cheng, and Z. H. Chen, J. Appl. Phys. **97**, 054102 (2005).
[12] J. Y. Chang, C. F. Chu, C. Y. Huang, and R. R. Yueh, J. Appl. Phys. **85**, 2318 (1999).
[13] F. Amy, A. S. Wan, A. Kahn, F. J. Walker, and R. S. Mckee, J. Appl. Phys. **96**, 1635 (2004).
[14] H. B. Lu, S. Y. Dai, F. Chen, L. Yan, Z. H. Chen, Y. L. Zhou, and G. Z. Yang, Ferroelectrics **271**, 125 (2002).
[15] G. Z. Yang, H. B. Lu, F. Chen, T. Zhao, and Z. H. Chen, J. Cryst. Growth, **227-228**, 929 (2001).
[16] H. B. Lu, K. -J. Jin, Y. H. Huang, M. He, K. Zhao, Y. L. Zhou, B. L. Cheng, Z. H. Chen, S. Y. Dai, and G. Z. Yang, Appl. Phys. Lett. **86**, 241915 (2005).
[17] B. H. Park, S. J. Hyun, C. R. Moon, B. D. Choe, J. Lee, C. Y. Kim, W. Jo, and T. W. Noh, J. Appl. Phys. **84**, 4428 (1998).
[18] Y. Li, L. Z. Hao, H. Deng, F. G. Chen, and Y. R. Li, J. Appl. Phys. **97**, 094103 (2005).
[19] K. Zhao, Y. H. Huang, Q. L. Zhou, K.-J. Jin, H. B. Lu, M. He, B. L. Cheng, Y. L. Zhou, Z. H. Chen, and G. Z. Yang, Appl. Phys. Lett. **86**, 221917 (2005).
[20] W. F. Zhang, Y. B. Huang, M. S. Zhang, and Z. G. Liu, Appl. Phys. Lett. **76**, 1003 (2000).
[21] J. I. Pankove, *Optical Processes in Semiconductors* (Prentice-Hall, New Jersey, 1971).